

PAPER • OPEN ACCESS

Characterization of prompt gamma rays for *in-vivo* range verification in hadron therapy: A Geant4 simulation study

To cite this article: M Zarifi *et al* 2019 *J. Phys.: Conf. Ser.* **1154** 012030

View the [article online](#) for updates and enhancements.

You may also like

- [Imaging of prompt gamma rays emitted during delivery of clinical proton beams with a Compton camera: feasibility studies for range verification](#)
Jeremy C Polf, Stephen Avery, Dennis S Mackin et al.
- [3D prompt gamma imaging for proton beam range verification](#)
E Draeger, D Mackin, S Peterson et al.
- [Carbon-11 and Carbon-12 beam range verifications through prompt gamma and annihilation gamma measurements: Monte Carlo simulations](#)
Ananta Raj Chalise, Yujie Chi, Youfang Lai et al.



ECS

Connect with decision-makers at ECS

Accelerate sales with ECS exhibits, sponsorships, and advertising!

▶ Learn more and engage at the 244th ECS Meeting!

Characterization of prompt gamma rays for *in-vivo* range verification in hadron therapy: A Geant4 simulation study

M Zarifi¹, S Guatelli¹, Y Qi¹, D Bolst¹, D Prokopovich² and A Rosenfeld¹

¹Centre for Medical Radiation Physics, University of Wollongong, Australia

²Australian Nuclear Science and Technology Organisation, Lucas Heights, Australia

E-mail: mz659@uowmail.edu.au

Abstract. Prompt gamma (PG) rays have been proposed for *in-vivo* beam range verification during treatment delivery. As a secondary by-product emitted almost instantaneously upon ion-nuclear interaction, PG rays offer real-time tracking of the Bragg peak (BP). However their detection is challenging since they have a broad energy spectrum with interference from neutrons and stray gamma rays. Numerous approaches have been proposed to utilise PG for *in-vivo* beam range verification. In this work, Geant4 Monte Carlo (MC) simulations have been used to study the spectral, spatial, temporal and angular distribution characteristics of PG emission and detection from hadron radiation fields of varying energy. Proton, ¹²C and ⁴He beams irradiated homogeneous water phantoms. These studies will provide valuable information for the development of clinically suitable and reliable PG detector systems.

1. Introduction

Hadron therapy is the use of charged particle beams to deliver targeted dose to tumours for radiation therapy treatment. Unlike conventional therapeutic photon beams, hadron beams penetrate the tissue with little scattering and deposit a maximum dose near the end of the ion range, with a sharp drop-off in dose that allows better sparing of the distal healthy tissue. The maximum dose distribution, termed the Bragg peak (BP), has the potential for conformed irradiation of the targeted region. However, precisely predicting and determining the BP position during treatment planning and delivery remains a challenge [1]. Prompt gamma (PG) rays offer a non-invasive *in-vivo* means for real-time monitoring of the ion dose delivery and range. PG rays are emitted almost instantaneously ($10^{-19} - 10^{-9}$ sec [2]) in the decay of excited nuclei arising from ion-nuclear interactions, and so they offer real-time BP tracking with high accuracy in the beam position.

The characteristics and feasibility of PG rays for *in-vivo* beam range verification have been studied, with a good correlation between the location and intensity of PG production and dose deposition observed. Detector designs have been explored for PG imaging (PGI), including mechanical collimation systems such as pinhole or knife-edge slit cameras [2, 3] and electronic collimation such as Compton cameras [4, 5]. Other beam monitoring techniques include PG spectroscopy (PGS) [6], PG timing (PGT) [7] and PG peak integration (PGPI) [8], which rely on the physical properties of PG rays such as energy and timing. The temporal properties of PG rays can not only be utilised for improving the signal-to-noise ratio in neutron rejection techniques [9], but also provide information on the beam position as it traverses the target [7]. Although advances for *in-vivo* range verification using PG rays have been made, the technology remains clinically unavailable, as PG detection is challenging due to the wide energy spectrum and strong interference background from



neutrons and other stray radiation. A recent study [8] showed a simple method of BP monitoring using the PG time-of-flight (TOF) peak mean and integral.

In this paper, we investigate the emission and detection characteristics of PG rays from water irradiated with particle beams of varying energy, with focus on the potential of employing the spectral and temporal properties of detected PG rays for un-collimated hadron beam range verification.

2. Materials and Methods

The Geant4 Monte Carlo toolkit [10] (version 10.02 patch 02) has been adopted to characterise PG emission and detection from hadron irradiation of a homogeneous water (H_2O , density of 1.0 g/cm^3) phantom. Mono-energetic pencil beams of proton and ^4He (62, 150, 200 and 250 MeV/u) and ^{12}C (120, 285, 385 and 490 MeV/u) were simulated. The phantom was cylinder in shape ($\phi 40 \text{ cm} \times 40 \text{ cm}$), positioned with its front face surface at the simulation coordinate centre, and the beam incident along the central axis of the phantom (along the z-axis), see figure 1. Particle depth-dose curves were obtained by calculating the energy deposited in the phantom along the z-axis. The PG emission time is the interval of time from the particle incidence on the phantom to the production of the gamma.

An ideal detecting sphere ($\phi 100 \text{ cm}$) surrounds the phantom, with its centre coinciding with the simulation coordinate centre, and registers gamma rays and neutrons that reach its surface once emitted from the phantom. The PG detection time, called *TOF*, is the interval of time from the particle incidence on the phantom to the detection of the secondary gamma/neutron at the detecting sphere.

The Geant4 physics included electromagnetic (standard_opt3 physics list) and hadronic physics (QGSP_BIC_HP for protons, neutrons and pions, Binary Ion Cascade models for ions). The Radioactive decay module of Geant4 was active. HP data libraries are adopted to model neutron interactions up to 20 MeV.

In the post-simulation data analysis, we quantify various parameters of the dose and PG emission/detection. We define the particle beam range *R* as the BP distal fall-off position, and the PG range R_{PG} as the PG emission yield fall-off position. TOF_{PG} is denoted as the PG TOF spectra peak fall-off. All fall-off values are taken at 80%. The angular distribution of PG rays was studied with the angle θ formed from the beam direction (z-axis) with the simulation coordinate centre. The maximum of a polynomial fitted to the distribution of θ values determines the preferential position *P* on the detecting sphere, whereby θ_{P} is the preferential polar angle. An energy threshold of 1 MeV is applied to all PG data, which eliminates low-energy photon counts that do not provide useful information for range verification.

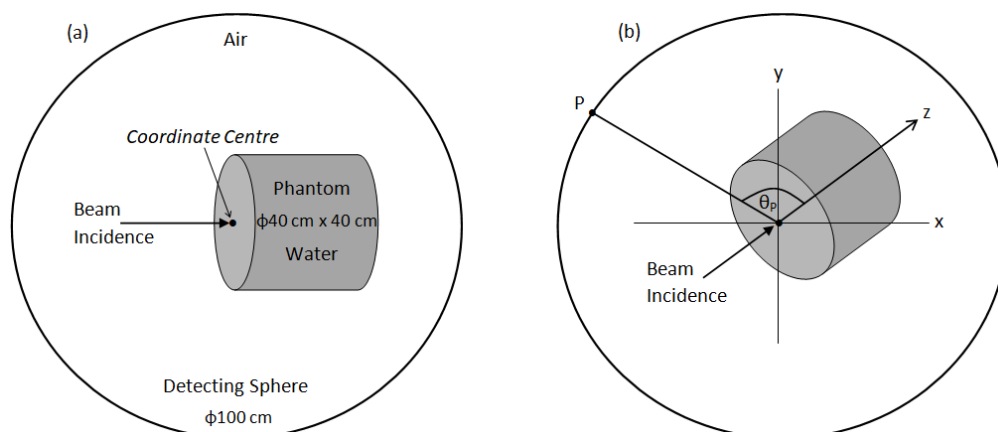


Figure 1. (a) Geometrical simulation setup. (b) The angle θ is formed from the z-axis with the coordinate centre, whereby θ_{P} is the preferential polar angle formed to the preferential position *P* on the detecting sphere determined with a polynomial fit in the post-simulation data analysis.

3. Results

For each of the particle beam types, the gamma energy spectra generated in the water phantom show characteristic PG emission peaks at 4.44, 5.21 and 6.13 MeV from the de-excitation of ^{12}C , ^{15}O and ^{16}O nuclei, respectively. A gamma peak at 511 keV represents annihilation photons, and a 2.22 MeV peak results from secondary thermal neutron capture by hydrogen. A strong spatial correlation between PG production and the dose profile was seen. The PG range accurately identifies the particle beam range: PG emission from heavier ions carbon and helium exhibit better accuracy (~ 2 mm) than the emission from protons (~ 6 mm). The time of emitted PG rays was also seen to vary with changing particle energy; with increasing beam energy PG rays are being produced at greater depths within the phantom and so generated at later times. Hence, the production time of PG rays correlates with the beam transit time and range.

The PG spatial distribution on the ideal detecting sphere showed isotropically azimuthal emission but non-isotropically axial emission such that the efficiency of PG detection can be maximised. Figure 2 compares θ_P values for PG rays from proton, ^{12}C and ^4He beams across the beam energies. θ_P is seen to become increasingly forward-peaked with increasing beam range, which suggests a dependence of the PG angular preferential position on the range depth with respect to the point of beam incidence. Analysis of gamma angular emission with respect to the BP position can be found in our previous study [11]. The TOF spectra of PG rays reaching the detecting sphere was also seen to depend on the particle beam range. As the beam energy increases, the TOF peak mean shifts to longer time values and the width/integral also increase, which is attributed to the greater distance of travel by the ions within the phantom, and hence the emission time of PG rays.

Figure 3 quantitatively compares the particle beam range and the corresponding PG range within the phantom, as well as PG TOF spectra data, for each particle type and energy. A good correlation is observed between R and R_{PG} . TOF_{PG} values increase gradually with increasing particle beam energy, with a slight decrease in the case for carbon beams at higher energies. Integral values of the TOF spectra exhibit a greater linearity with increasing beam energy and thus particle range. Heavier ion irradiations, such as carbon, may present a greater challenge for employing the PG TOF information for range monitoring due to the greater influence of background gamma rays such as those produced in the dose tail of the carbon beam as a result of nuclear fragmentation reactions.

Neutrons were seen to be predominantly emitted in the forward direction with longer TOF values compared to PG rays, which suggests two means (position of the detection system and timing properties of the detector) for discriminating PG rays from the interference background and hence improve the signal-to-noise ratio of PG detection.

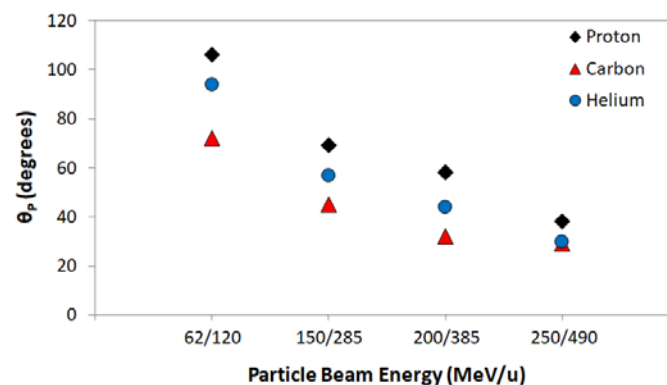


Figure 2. Preferential polar angle θ_P for PG detection, for protons and ^4He ions (62-250 MeV/u) and ^{12}C ions (120-490 MeV/u). An energy threshold of 1 MeV is applied to the PG data. The uncertainty of θ_P values is estimated around 1° .

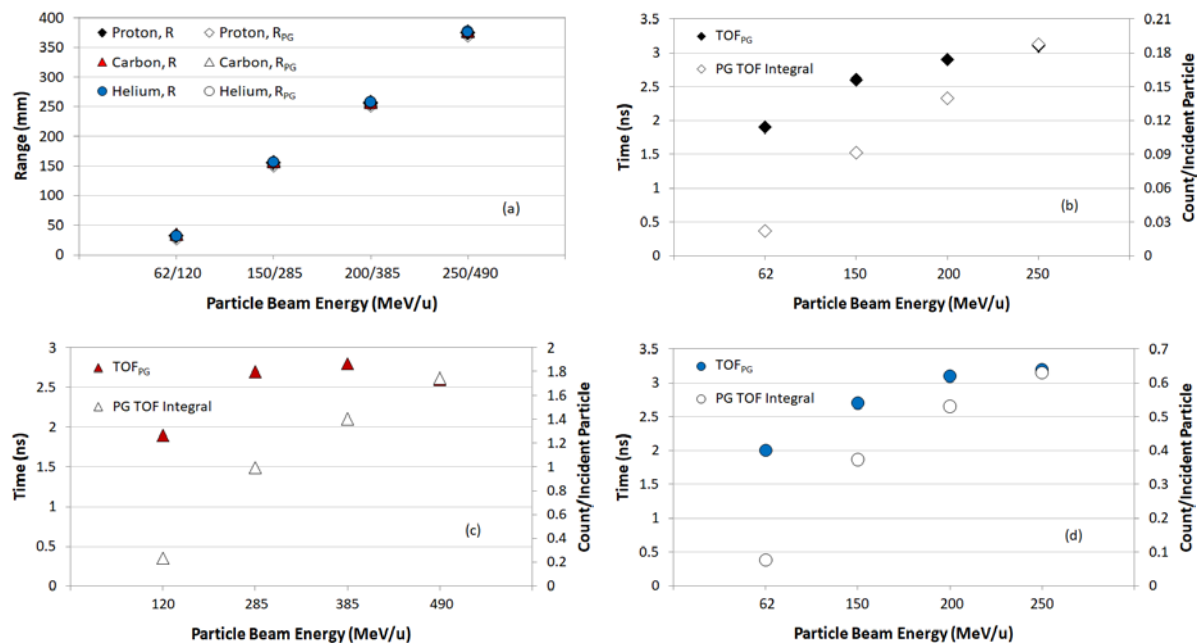


Figure 3. Quantitative data for (a) correlation between R and R_{PG}, and (b)-(d) TOF_{PG} and TOF peak integral count per incident particle, for protons, ^{12}C and ^4He ions, respectively. An energy threshold of 1 MeV is applied to the PG data. The uncertainty of range values is 0.1 mm and time values is 0.1 ns. The simulation statistical uncertainty affecting the count values is within 1%.

4. Conclusion

The emission and detection characteristics of PG from hadron irradiations of a water phantom were studied. Our results show that there is a preferential axial angular position for improving the efficiency of PG detection which depends on the beam energy relative to a fixed point of reference, such as the phantom surface. The range and emission time of PG rays produced within the phantom correlate to the particle beam range. As the PG emission time depends on the beam transit time, the PG TOF spectrum is also seen to change with particle range, suggesting a potentially simpler technique of beam range verification using un-collimated PG timing data. Further investigations into this technique for hadron therapy range verification are underway.

5. References

We would like to thank the University of Wollongong Information Management & Technology Services (IMTS) for computing time on the UOW High Performance Computing Cluster. This research has been conducted with the support of the Australian Government Research Training Program Scholarship

6. References

- [1] Gorjiara T *et al* 2012 *Med. Phys.* **39** 7071-9
- [2] Smeets J *et al* 2012 *Phys. Med. Biol.* **57** 3371-405
- [3] Min C H *et al* 2006 *Appl. Phys. Lett.* **89** 183517
- [4] Richard M H *et al.* 2011 *IEEE Trans. Nucl. Sci.* **58** 87-94
- [5] Peterson S W *et al* 2010 *Phys. Med. Biol.* **55** 6841-56
- [6] Verburg J M and Seco J 2014 *Phys. Med. Biol.* **59** 7089-106
- [7] Golnik C *et al* 2014 *Phys. Med. Biol.* **59** 5399-422
- [8] Krimmer J *et al* 2017 *Appl. Phys. Lett.* **110** 154102
- [9] Biegun A K *et al* 2012 *Phys. Med. Biol.* **57** 6429-44
- [10] Agostinelli S *et al.* 2003 *Nucl. Instrum. Methods Phys. Res. A.* **506** 250-303
- [11] Zarifi M *et al* 2017 *Phys. Med.* **33** 197-206